

# Observational constraints on particle production during inflation

Yrstein Elgarøy

NORDITA, Blegdamsvej 17, DK-2100 Copenhagen, Denmark

Steen Hannestad

Department of Physics, University of Southern Denmark, Campusvej 55, DK-5230

Odense M, Denmark

and

NORDITA, Blegdamsvej 17, DK-2100 Copenhagen, Denmark

Troels Haugbølle

Department of Astronomy, Niels Bohr Institute,

Juliane Maries Vej 30, DK-2100 Copenhagen, Denmark

**Abstract.** Resonant particle production, along with many other physical processes which change the effective equation of state (EOS) during inflation, introduces a step-like feature in the primordial power spectrum. We calculate observational constraints on resonant particle production, parameterised in form of an effective step height,  $N_e$  and location in  $k$ -space,  $k_{\text{break}}$ . Combining data from the cosmic microwave background and the 2dF Galaxy Redshift Survey yields strong constraints in some regions of parameter space, although the range in  $k$ -space which can be probed is restricted to  $k \approx 0.001 - 0.1 \text{ h Mpc}^{-1}$ . We also discuss the implications of our findings for general models which change the effective EOS during inflation.

PACS numbers: 14.60Pq, 95.35.+d, 98.80.-k

## 1. Introduction

The recent measurements of the temperature anisotropies in the cosmic microwave background (CMB) from the Wilkinson Microwave Anisotropy Probe (WMAP) [1, 2, 3, 4, 5] have set a new standard for precision in cosmology. In addition to pinning down several key cosmological parameters with unprecedented accuracy, the WMAP data have confirmed important aspects of the inflationary paradigm. Quantum fluctuations during the inflationary phase are commonly thought to be the seeds of the anisotropies in the CMB and large-scale structure in the Universe. The observations are consistent with the inflationary mechanism for generating curvature fluctuations on superhorizon scales, and with the fluctuations being adiabatic and Gaussian as in the simplest single-field models [6]. The fluctuations are conveniently characterized by the power spectrum of the curvature perturbations  $P_R(k)$ , and in the simplest models it is proportional to some power of the comoving wavenumber  $k$  of a given Fourier mode,  $P_R(k) \propto k^{n_s - 1}$ , where  $n_s$  is the so-called scalar spectral index. For  $n_s = 1$  one has the case of scale-invariant fluctuations. The data favour a slight red tilt of the scalar spectral index,  $n_s < 1$ , again consistent with single-field models [2].

However, there are several possible extensions to the simplest models for inflation, and in most of them deviations from the simple power-law form of the primordial power spectrum are produced. Models which produce features in the primordial power spectrum include variants of extended inflation [7], models with multiple episodes of inflation [8], and phase transitions during the inflationary phase [9]. In this paper we consider another proposal, resonant particle production during inflation, which extends the single-field models by coupling the inflaton to a massive field (see e.g. [10]). By this mechanism energy can be extracted from the inflaton field during inflation, altering its classical motion and producing features in the primordial power spectrum.

Our aim in this paper is to calculate in detail the shape of the primordial power spectrum in the presence of resonant particle production, and to constrain this class of models using a collection of the latest cosmological data, including the WMAP CMB power spectrum and the 2dF Galaxy Redshift Survey (2dFGRS) galaxy power spectrum [11]. It is important to bear in mind that  $P_R(k)$  is not directly observable. Whether we look at the CMB or the large-scale distribution of matter, what we see is the primordial fluctuations modified by astrophysical processes. Thus, our ability to constrain the primordial fluctuations depends on our understanding of the physics involved in the processing, and on our knowledge of the relevant parameters controlling the physics, for instance the matter density. Combining different cosmological observations is therefore essential, since different observations probe different combinations of cosmological parameters and thus combining them breaks parameter degeneracies and allows tighter constraints to be obtained.

The structure of this paper is as follows. In section 2 we describe the model and the calculation of the primordial power spectrum in the presence of resonant particle production, and in section 3 we comment on the generality of our results. The

observations we use, CMB data and the galaxy power spectrum, are described in section 4, and section 5 discusses the likelihood analysis and the results, before we conclude in section 6.

## 2. Resonant particle production

We will work with the simplest possible single field model. We do this because, as will be seen, the main interest here is not the slow change in the power spectrum during the course of inflation, but rather, what happens if a resonant phenomenon (namely a sudden burst of particle production) radically changes the dynamics for a short period of time.

Our specific toy model is that of a single scalar field, dubbed the inflaton, and which is rolling slowly down its potential in accordance with the slow-roll conditions, dominating the energy (momentum) tensor. The inflaton is coupled through the mass to a massive boson  $\chi$  in such a way that at a certain moment  $t_0$   $\chi$  becomes massless. Initially  $\chi$ , being heavy compared to the natural mass scale set by the expansion rate  $m_{\text{natural}}^2 \chi^2$ , is in its vacuum state. The potential is

$$V(\phi; \chi) = V(\phi) + \frac{1}{2} N (m - g \phi)^2 \chi^2; \quad (1)$$

where we will allow for the case where  $\chi$  represent some degenerate species and we denote the number of different species by  $N$  as done in [10]. The phenomenon is strongly resonant essentially because any particles created will be red shifted away exponentially fast.

To find the backreaction we will treat the inflaton at the classical level, while the  $\chi$  field is fully quantised. Computing the backreaction implies finding the expectation value of the energy (momentum) tensor associated with the  $\chi$  field. This is, due to problems with proper regularisation and renormalisation, a highly nontrivial problem (see e.g. [24, 20, 22] and [18, 19] for the fermionic case), but as a lowest approximation we can use the Hartree approximation.

### 2.1. Formalism and equations of motion

We assume a spatially flat Friedmann-Robertson-Walker (FRW) model overlaid with linear scalar perturbations and the metric takes the form [25]

$$ds^2 = (1 + 2A) dt^2 + 2a(t) \partial_i B dx^i dt + a^2(t) [(1 - 2C)_{ij} + 2\partial_i \partial_j E] dx^i dx^j \quad (2)$$

where  $a(t)$  is the scale factor and  $A$ ,  $B$ ,  $C$ , and  $E$  describes the possible scalar metric perturbations. Likewise any scalar field  $\phi$  can be split in a homogeneous part and a fluctuation

$$\phi(t; \mathbf{x}) = \bar{\phi}(t) + \delta\phi(t; \mathbf{x}) \quad (3)$$

Because of the inherent gauge freedom related to the arbitrariness of coordinates, we can eliminate two out of the four metric perturbations by choosing the spatial and temporal hypersurfaces in a proper way [17, 21].

The physical content is of course not changed by such a coordinate or gauge transformation. Certain algebraic combinations of the metric and matter perturbations in any gauge can be found that corresponds to a certain perturbation in a specific gauge. These combinations are dubbed gauge invariant variables. In this paper we will use the spatially flat gauge to describe the field perturbations. These are called the Sasaki-Mukhanov variables:

$$Q_I = \delta\phi_I + \frac{\dot{\phi}_I}{H} \quad (4)$$

Their evolution equations are [23]

$$Q_I''(k) + 3H Q_I'(k) + \frac{k^2}{a^2} Q_I(k) + M_{IJ} Q_J(k) = 0; \quad (5)$$

where  $M_{IJ}$  is the effective mass matrix

$$M_{IJ} = V_{IJ} - \frac{8}{m_{pl}^2 a^3} \frac{a^3 \dot{\phi}_I \dot{\phi}_J}{H} \quad (6)$$

and  $V_{IJ}$  denotes  $\partial^2 V = \partial_I \partial_J V$ .

A popular measure of the curvature perturbation, which later directly relates to the temperature perturbation in the CMBR, is  $R$  the spatial curvature seen by observers who are comoving with the energy content. It is conveniently related to the Sasaki-Mukhanov variables as [26]

$$R = H \frac{-\dot{\phi}_I}{\dot{\phi}_I} Q_I \quad (7)$$

The evolution of the background parameters, taking into account the backreaction of the field, but not rescattering of the inflation field itself is found to be:

$$\dot{H} = 3H - \frac{dV(\phi)}{d\phi} + gN(\dot{\phi})^2 \quad (8)$$

$$H^2 = \frac{8}{3m_{pl}^2} \left[ \frac{1}{2} \dot{\phi}^2 + V(\phi) \right] + \frac{1}{2} N \dot{\phi}^2 + \frac{1}{2} N (g \dot{\phi})^2 + \frac{1}{2a^2} h r'^2 \quad (9)$$

$$\dot{H} = -\frac{4}{m_{pl}^2} \left[ \frac{1}{2} \dot{\phi}^2 + h r'^2 \right] + \frac{1}{3a^2} h r'^2 \quad (10)$$

The expectation values  $h r^2$  will be computed below.

## 2.2. Quantisation of the field

When we quantise the field we will disregard any effects arising from the metric perturbations. This is reasonable as long as we are looking at wavelengths shorter than the horizon size. We will see below that indeed the bulk of the energy is deposited in subhorizon modes justifying the approach. The backreaction of modes on the field can also be disregarded, because it is an almost homogeneous light field.

Working in the Heisenberg picture the field can be canonically quantised and decomposed in terms of annihilation and creation operators. We have chosen to use the

rescaled field  $a^{3=2}$ . This is done in order to get rid of trivial prefactors arising from the expansion of background space{time}.

$$a^{3=2} \hat{\alpha} = \frac{1}{(2)^{3=2}} \int d^3k \hat{\alpha}_k a^{3=2}{}_{,k}(t) e^{ikx} + \hat{\alpha}_k^y a^{3=2}{}_{,k}(t) e^{+ikx} \quad (11)$$

satisfying the usual commutation relations

$$[\hat{\alpha}_k; \hat{\alpha}_{k^0}] = [\hat{\alpha}_k^y; \hat{\alpha}_{k^0}^y] = 0; \quad [\hat{\alpha}_k; \hat{\alpha}_{k^0}^y] = \delta^3(k - k^0) \quad (12)$$

By construction  $\hat{\alpha}_k$  has to be a solution to the classical Klein Gordon equation of a massive field with time dependent mass

$$a^{3=2}{}_{,k} + !_k^2 a^{3=2}{}_{,k} = 0; \quad (13)$$

$$!_k^2 = \frac{k^2}{a^2} + (m - g)^2 - \frac{9}{4}H^2 - \frac{3}{4}H^2; \quad (14)$$

Except for the very small time interval in which the particles are produced, the field is heavy compared to the "Hubble mass"

$$(m - g)^2 - \frac{3}{2}H^2 \quad (15)$$

and the vacuum fluctuations are exponentially damped on large scales. When  $(m - g)^2 < \frac{3}{2}H^2$  particle production occurs, and we can assume it to be the dominant effect. Therefore we will disregard vacuum polarization altogether. To understand the qualitative behaviour of the dynamics, we do not need to include the terms coming from the metric (6) nor terms in (14) that are dependent on the Hubble parameter.

Initially  $\hat{\alpha}_k$  is in the vacuum state of a heavy bosonic field

$$a^{3=2}{}_{,k} = \frac{1}{\sqrt{2!_k}} e^{i \int_{t_0}^t R_t !_k dt} \quad (16)$$

while after some moment  $t_0$ , where

$$m - g_0 = 0; \quad (17)$$

particle production, because of interaction with the inflaton, has occurred. Generally  $\hat{\alpha}_k$  can be written in terms of "adiabatic" solutions to (13)

$$a^{3=2}{}_{,k}(t) = \frac{1}{\sqrt{2!_k}} e^{i \int_{t_0}^t R_t !_k dt} + \frac{1}{\sqrt{2!_k}} e^{+i \int_{t_0}^t R_t !_k dt} \quad (18)$$

Then initially  $!_k = 1; !_k = 0$ , while at later times the effective mass  $(m - g)$  only changes slowly and (18) is a solution to (13) with constant  $!_k, !_k$ .

### 2.3. Characteristics of the $\hat{\alpha}$ field

Choosing a special boundary condition for (13) is equivalent to singling out a special set of observers (and annihilation and creation operators). We have already mentioned one, namely (16), which is related to the vacuum seen by observers in the infinite past. Another interesting vacuum is the comoving vacuum related to the observers which are comoving at a given time.

Different vacua are related to each other by a Bogoliubov transformation

$$\hat{\alpha}_k(t) = \alpha_k' \hat{\alpha}_k(t) + \beta_k' \hat{\alpha}_k^\dagger(t) \quad (19)$$

We can from this transformation directly calculate distribution functions and expectation values of a field in the  $\hat{U}$  vacuum state, seen by an observer corresponding to the  $\hat{0}$  vacuum state. Notice that as a consequence of our parametrisation (18), we can read off the Bogoliubov coefficients for a transformation from the initial vacuum state to a comoving state to be  $\alpha_k; \beta_k$  as defined in (18).

If we suppose that the particle production is resonant around  $t_0$ , the effective mass of  $\psi$  can be Taylor expanded near  $t_0$ . Furthermore if everything happens approximately during one e-fold we will also assume  $a \approx a_0$  and the equation of motion for the  $\psi$  modes (13) in this neighbourhood is

$$a^{3=2} \ddot{\alpha}_k + \left( \frac{k^2}{a_0^2} + g^2 j_0 j_0 (t - t_0)^2 \right) a^{3=2} \alpha_k = 0; \quad (20)$$

Now we can rewrite (13) in terms of the dimensionless momentum  $p^2 = k^2/a_0^2$  and the time  $T^2 = (t - t_0)^2$ , where  $\tau = g j_0 j_0$

$$\frac{d^2}{dT^2} a^{3=2} \alpha_p + p^2 + T^2 a^{3=2} \alpha_p = 0 \quad (21)$$

This is equivalent to a Schrodinger equation for scattering at a (negative) parabolic potential and can be solved in terms of parabolic cylinder functions. The incoming wave can be approximated as pure positive frequency corresponding to being in the vacuum state, while the outgoing state  $(\alpha_k; \beta_k)$  is found to be (see [24] for details)

$$\alpha_k^{out} = \frac{1}{1 + e^{-p^2}} e^{i k}; \quad \beta_k^{out} = \frac{i e^{-\frac{1}{2} p^2}}{2} e^{2i k} \quad (22)$$

$$\arg \alpha_k = \arg \frac{1 + i p^2}{2} + \frac{p^2}{2} \ln \frac{p^2}{2} \quad (23)$$

The number density of  $\psi$  modes after particle production is given as [20]

$$\begin{aligned} a^3 n_k(t) &= \langle \hat{N}_k \rangle = \langle \hat{\alpha}_k^\dagger(t) \hat{\alpha}_k(t) \rangle \\ &= |j_k^{out}|^2 = e^{-p^2} = e^{-\frac{k^2}{g j_0 j_0 a_0^2}} \end{aligned} \quad (24)$$

If we suppose the typical time scale of the inflation field is  $H^{-1}$  then  $\tau \approx H_0$ . From the slow-roll result and the limit on the quadrupole we find that if particle production has happened at an observationally interesting scale, the exponent above becomes  $\frac{H_0}{m} \left( \frac{k=a_0}{H_0} \right)^2$ . This goes to show that initially the spectrum of  $\psi$  modes will be quite blue. Integrating (24) we find the total number density to be

$$n_\psi(t) = \frac{1}{(2\pi)^3} \int dk^3 n_k = g^{3=2} \frac{j_0 j_0^{3=2}}{(2\pi)^3} \frac{a_0^{-3}}{a_0} n_0 \frac{a_0^{-3}}{a_0} \quad (25)$$

When we try to calculate the two-point correlator  $\langle h^2 \rangle$  ultraviolet divergences arise. These can be dealt with exactly like in normal flat Minkowski space by subtracting the  $z$ . Strictly speaking this is only true for vacua which share the same spatial base [20].

vacuum contribution [10] and we find

$$\begin{aligned}
 \langle h'^2 \rangle &= \frac{1}{2^2 a^3} \int \frac{d^3 k}{(2\pi)^3} \langle j_k j_k \rangle + \text{Re} \left( \int \frac{d^3 k}{(2\pi)^3} e^{2i \int_{t_0}^t k dt} \right) \\
 &= \frac{C}{m^2 g} n_0 \frac{a}{a_0}^3 ; \tag{26}
 \end{aligned}$$

where  $C = 0.680$  is a numerical constant.

#### 2.4. The inflation field

Energy from the created  $\chi$  particles are draining the kinetic energy of the background inflation field, but in turn the  $\chi$  field reacts back on the fluctuations of the inflation. The inflation field is a light field, it is frozen on large scales, and it is important to use the full equation of motion (5) including metric terms for its fluctuations  $Q_k$ .

The homogeneous part of the  $\chi$  field is negligible to begin with, because the field is overdamped on large scales. If this is the case, and we later disregard oscillations between the two fields, i.e. correlators of the form  $\langle h' \chi \rangle$ , then the homogeneous part of the  $\chi$  field is easily seen to remain negligible. This in turn means, we can disregard any off-diagonal terms in the equation of motion for the fluctuations of the  $\chi$  field. Their equation of motion, using (5), is then

$$Q_k = -3H\dot{Q}_k - \frac{k^2}{a^2} Q_k + \frac{d^2 V(\phi)}{d\phi^2} Q_k + g^2 N \langle h'^2 \rangle \tag{27}$$

$$+ \frac{8}{m_{pl}^2 H} \left( 3H + \frac{\dot{H}}{H} \right) Q_k - 2 \frac{dV(\phi)}{d\phi} g N (m - g) \langle h'^2 \rangle Q_k ; \tag{28}$$

where we naively have replaced any quadratic terms in  $\chi$  with the corresponding correlators.

In a proper treatment one should of course include other higher order terms both in (27) and (8) coming from metric terms [17, 21, 29, 28, 27], but most probably it will only lead to a quantitative change of the produced feature in the power spectrum, not a qualitative one.

#### 2.5. Numerical results

In order to find the impact on the power spectrum, we carried out a numerical integration of the whole system including the two point correlators such as the one in (26). The obvious strategy would be to evaluate the two point correlators in terms of the Bogoliubov coefficients, but this scheme turns out to be numerically unstable. Instead we use the idea of [22] and parameterise  $\chi_k$  as

$$\chi_k = \frac{e^{i \int_{t_0}^t k dt}}{2! k a^{3-2}} [1 + f] \tag{29}$$

$$\langle \chi^2 \rangle = \int \frac{d^3 p}{(2\pi)^3} \int \frac{d^3 p'}{(2\pi)^3} (1 + e^{i \int_{t_0}^t p' dt}) \langle \chi_{p'} \chi_{p-p'} \rangle$$

Making  $f$  the dynamical variable we get the advantage that the two-point correlators can be evaluated directly in terms of  $f$ . In contrast, evaluating the correlators directly in terms of  $'_k$  or the Bogoliubov coefficients involve differences between  $'_k$  and  $'_{-k}$ , two highly oscillating functions prone to numerical instability. After some algebra, we find all the two-point correlators:

$$h'^2_i = \frac{1}{2^2 a^3} \int^z \frac{k^2 dk}{!_k} \frac{1}{2} \overline{f} f + \text{Re}(f) \quad (30)$$

$$h'_{-i} = \frac{1}{4^2 a^3} \int^z \frac{k^2 dk}{!_k} \text{Re}((1+f)\overline{f}) \left( \frac{!_k}{2!_k} + \frac{3}{2} H^2 \right) (\overline{f} f + 2\text{Re}(f)) \quad (31)$$

$$\begin{aligned} h_{-i}^2 = & \frac{1}{4^2 a^3} \int^z \frac{k^2 dk}{2!_k} \overline{f} f + \frac{!_k}{2!_k} + \frac{3}{2} H^2 + !_k^2 \overline{f} f + 2\text{Re}(f) \\ & + 2\text{Re}(f) !_k \text{Im}(f) (1 + \text{Re}(f)) \left( \frac{!_k}{2!_k} + \frac{3}{2} H^2 \right) \\ & + 2\text{Im}(f) !_k (1 + \text{Re}(f)) + \frac{!_k}{2!_k} + \frac{3}{2} H^2 \text{Im}(f) \quad (32) \end{aligned}$$

Notice that in all of the above expressions the  $t=0$  contribution from the vacuum expectation value has been subtracted, rendering them finite.

Inserting the definition of  $f$  (29) in (13) we find its evolution equation

$$\dot{f} = -2i!_k + \frac{!_k}{!_k} \overline{f} - \frac{3}{4} \frac{!_k}{!_k} \int^z \frac{!_k}{2!_k} \frac{9}{4} H^2 - \frac{3}{4} H^2 (1+f) \quad (33)$$

To make any actual integration we have to choose a specific inflationary model by specifying the inflation potential  $V(\phi)$ . For ease of comparison, we have chosen to use the same model as Chung et al. [10]:

$$V(\phi) = \frac{1}{2} m^2 \phi^2; \quad m = 10^6 m_{\text{pl}}; \quad m = 2m_{\text{pl}}; \quad g = 1 \quad (34)$$

with varying  $N$ . To check if the slope of the slow-roll potential had any impact, several runs with the exponential potential

$$\begin{aligned} V(\phi) = & \frac{1}{2} m^2 m_{\text{pl}}^2 \exp\left(-\frac{\phi}{m_{\text{pl}}}\right); \quad \alpha = 0.7034; \\ & m = 10^6 m_{\text{pl}}; \quad m = 2m_{\text{pl}}; \quad g = 1 \quad (35) \end{aligned}$$

were carried out. The value of  $\alpha$  and  $m$  are chosen such that  $\alpha$  and the Hubble parameter  $H$  are exactly the same as in (34) at the moment of particle production. This potential is ideally suited to test if the inflation potential has any impact, because it has a substantially higher acceleration of the inflation. We found that the effective step height  $N_{\text{eff}}$  is virtually unaltered between the two models, confirming the resonant nature of the phenomena.

By starting the simulation at a point so far back in time that all modes of interest were way inside the horizon, we used the Bunch-Davies vacuum state (16) as initial values for  $'_k$  and  $Q_k$ . Furthermore the inflation was taken to be slow-rolling:

$$\dot{\phi}(0) = -\frac{V_{,\phi}(\phi_{\text{start}})}{3H(\phi_{\text{start}})} \quad H^2(0) = \frac{8}{3m_{\text{pl}}^2} V(\phi_{\text{start}}) \quad (36)$$

$$Q_k(0) = \frac{e(k)}{2ka^{3/2}} \quad Q_k(0) = \frac{3}{2}H + i\frac{k}{a_0} Q_k(0) \quad (37)$$

$$f = 0 \quad \dot{f} = 0; \quad (38)$$

where  $e(k)$  is a random variable on the complex unit circle. To check that these values had no impact on the further evolution, different starting values  $Q_{\text{start}}$  were chosen for different runs, and in general  $a_{\text{start}}$  was tuned such that at  $m_{\text{pl}} g_0 = 0$  we have  $a_0 = 1$ . To get the proper attractor solution of the background inflation field, we let the simulation run for some initial time until the slow-roll solution has relaxed to the correct attractor one. Afterwards we start evolving the  $\delta\phi$  and  $\delta\psi$  modes.

Comparison between the analytical approximations and numerical computation of the time evolution of the two-point correlator  $\langle \delta\phi^2 \rangle$  has been made with excellent agreement (see figure 1). Notice in figure 1 the very steep decline in the correlation function just at the beginning. We interpret it as the first short time span, where the particles are relativistic. If we look at the approximation (26) for the correlation function it is singular in the beginning, because we, in making the approximation, have neglected the  $k$ -dependence of the energy  $\epsilon_k$ . Obviously we have to take that into account when  $H_0 t \ll 1$ . We then find

$$\langle \delta\phi^2 \rangle_{\text{REL}} \approx \frac{1}{2} \frac{1}{a^2} \int dk k^3 \langle \delta\phi^2 \rangle = \frac{2n_0}{g_{\text{eff}}} \frac{a}{a_0} \quad (39)$$

If we now, inspired by the form of  $\epsilon_k$ , make an ansatz for the correlation function of the form

$$\langle \delta\phi^2 \rangle = \frac{n_0}{g_{\text{eff}} t^2} \frac{a}{a_0} \quad (40)$$

we find, by comparison with (26) and (39) and taking the appropriate limits, that

$$H_0 t_c = \frac{H_0}{2 g_{\text{eff}}} \quad (41)$$

Equation (40) is plotted together with the numerical result in figure 1. We can interpret  $H_0 t_c$  as the number of e-folds where on average the energy of the produced particles is stored in relativistic modes. Because of the CMBR limit on the quadrupole, and recalling the slow-roll result, in any model of single field inflation we will have  $H_0 t_c \approx 10^3 g^{-1/2}$ .

It is important to confirm the findings of [10], that the analytic approximation for the Bogoliubov coefficients are very precise. The number density  $n_k$  is plotted in figure 1 and shows excellent agreement. Notice that at relatively high  $k$  values, compared to the horizon size, the number density is still significant. The energy density at the moment of particle production per logarithmic interval scales as  $k^3 n_k$  and therefore the peak energy occurs at values much larger than  $H_0$ . This means that the process by far and large is local in nature and the impact from the expanding background is small. It assures us that even though we have neglected all the metric backreaction terms, we still get a result which at least qualitatively agrees with what a proper treatment would yield.

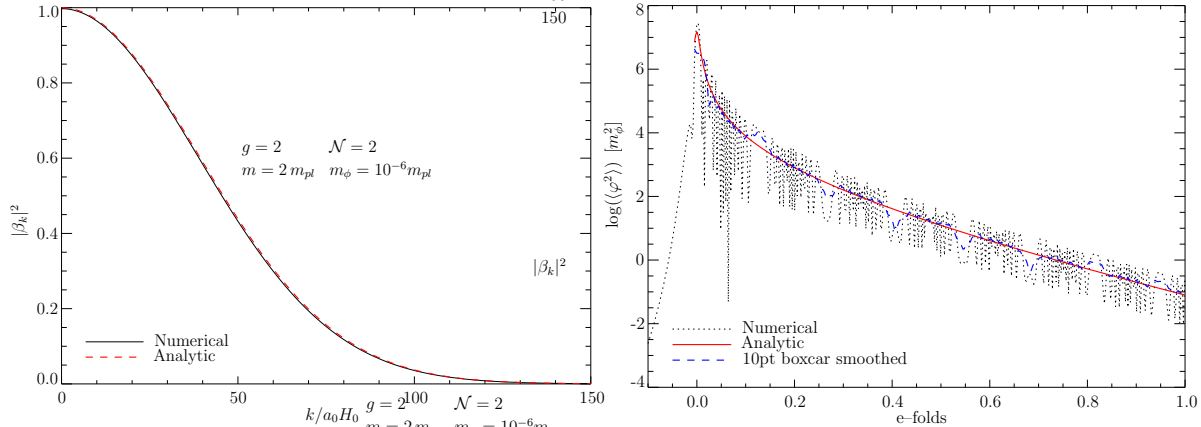


Figure 1. The number density and the time development of the correlation function, which roughly speaking is the same as the backreaction term. Both are compared to the analytic approximations, and in general there are very good agreement. The boxcar smoothing, was done to emphasise the secular evolution by canceling out the oscillations.

In general our results for the background parameters such as the inflation velocity and the Hubble parameter are very much in line with [10] and we will not repeat their analysis here. The reason is that the detailed evolution of the inflation or the Hubble parameter  $H$  do not have a direct observable impact. They would only be needed if we wanted to do a detailed analytical modeling.

## 2.6. The curvature perturbation

The essential quantity to consider is the comoving curvature perturbation  $R$ . It is found to be in qualitative disagreement with any analytic prediction, regardless of whether we use the slow roll [14], the Stewart-Lyth [15] or even the semi-numerical method of Leach et al. [16]. They all fail because they assume the impact of any change in the fields or fluctuations is local in the sense that it only affects modes which are just about to cross the horizon. However, this is not the case if the entropy perturbation is changing [13, 26], and this is exactly what happens. The homogeneous inflation field suddenly dumps a huge amount of energy into ultra relativistic particles. It leads to a suppression of the comoving curvature perturbation on all scales larger than the horizon, and the formation of a step in the potential (see figure 2).

On top of the main feature, the step in the potential, there are high frequency oscillations. As is obvious from the graph, the frequency increases with increasing wave number  $k$ . This suggests a qualitative interpretation, from a mathematical point of view, of both the step and the oscillations. The comoving curvature perturbation  $R$  is related to the inflation field fluctuation  $Q_k$  according to equation (7), while the power spectrum is defined in the usual way

$$P_R^{l=2} = \frac{1}{2} \frac{k^3}{2} \mathcal{R}^2 \quad (42)$$

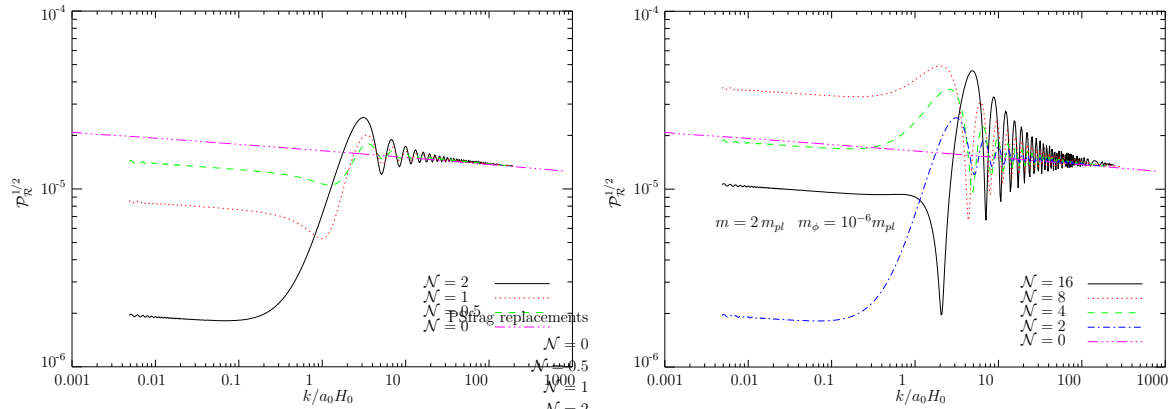


Figure 2. The power spectra from different models. In the right plot the effective number of degrees of freedom is so high that a perturbative calculation of the step height cannot be trusted, while the left plot shows the monotonic evolution of step height for weaker couplings.

To understand features in  $P_R$  we can equally well analyse  $Q_k$ , because the change in  $H$  is negligible and the change in  $\dot{\phi}$  is only transient (see equation (7)).

While inside the horizon a single perturbation with definite wave number  $k$  is oscillating with a frequency that approximately is given as  $k=a$  (for a massless field). At the moment of particle production we can schematically write the equation for this mode  $Q$  as

$$Q + 3H \dot{Q} + \frac{k^2}{a^2} Q + B(t) Q = 0; \quad (43)$$

where  $B(t)$  is the backreaction term. Now depending on the phase of  $Q$  at the exact moment of particle production the final amplitude will either be increased or decreased [12] (see second plot in figure 2). Inside the horizon the phase is highly oscillating  $Q \sim \exp(ik=at)$  and we get wiggles on the UV part of the spectrum. Modes which are far outside the horizon have approximately  $k=a=0$  and the amplitude change very slowly, therefore they all experience the same kick from  $B(t)$  making the step in the potential.

In the short interval, where  $B^{1=2}(t)$  is greater than the Hubble mass  $3=2H$ , the superhorizon modes begin to oscillate again. In the perturbative regime this "oscillation" lasts for such a short time that the modes do not even cross zero a single time, and we can compute the impact using simple perturbation theory. On the other hand, if  $B(t)$  is large enough, zero-crossing occurs and effectively the impact from  $B(t)$  is larger than the starting amplitude and perturbative methods become meaningless.

Let us define the effective step height  $N_{\text{eff}}$  as the quotient between the ultraviolet and the infrared part of the power spectrum  $P_R^{1=2}$ , which is the main observational signature. For small values of the coupling it is possible to make an analytic approximation for  $N_{\text{eff}}$ . This is very valuable, because it enables us to connect the inner parameters of the theory, i.e. the coupling, the effective degrees of freedom etc, to the observable: The effective step height  $N_{\text{eff}}$ .

For low  $k$  values, until the particle production starts,  $Q_k$  is evolving very slowly and can be taken to be constant. Then, suddenly, particle production commences. The main term in the equation of motion for  $Q_k$  (27) is the two point correlation function. Define the rescaled mode  $\mathcal{Q} = a^{3-2\epsilon} Q$  and use e-folds  $N$  as time variable, then approximately

$$\frac{d^2 \mathcal{Q}}{dN^2} + g^2 N \frac{h^2 i}{H^2} \frac{9}{4} \mathcal{Q} = 0 \quad (44)$$

and the boundary conditions are, still for low  $k$  values only,

$$\mathcal{Q}(0) = \mathcal{Q}_0 \quad \frac{d\mathcal{Q}}{dN}(0) = \frac{3}{2} \mathcal{Q}_0 \quad (45)$$

Unfortunately, inserting the expression (40) for the correlation function, we get an equation without analytical solutions. But we can exploit the fact that the integrated impact of the correlation function is supposed to be small. Then the exact functional form is not so important only the integrated size and instead of the correlation function can we substitute an exponential  $A e^{3N}$  with the correct late time behaviour. The equation can now be solved in terms of Bessel functions and plugging in the boundary conditions we get the late time behaviour and can evaluate the effective step height

$$N_{\text{eff}} = 1 - \frac{1}{9} A + \frac{1}{324} A^2 + \dots \quad (46)$$

$A$  can be determined by the requirement that the integrated size of the perturbation has to be the same as for the correlation function:

$$\int_0^{z_1} A e^{3N} dN = g^2 N \int_0^{z_1} \frac{h^2 i}{H^2} dN \quad (47)$$

$$A = 3g^{5-2\epsilon} N \frac{z_1}{(2)^3 H_0^3} \ln \frac{2}{3H_0 t_c} e^{+3H_0 t_c} ;$$

where  $e^{-\gamma} = 0.577$  is Euler's constant and we have evaluated the integral to first order in  $H_0 t_c$ . The result is in agreement with the numerics.

### 3. Models with a changing EOS

The previous section shows that the impact on the curvature perturbation on large scales is a generic feature. It has to do with the rapid change of the potential energy or, alternatively, of the equation of state. We find our result in agreement with analyses of similar models, all possessing the property of having a sudden change in the EOS.

Starobinsky [35] constructed a phenomenological model, where the potential has a break in its slope. Roberts et. al [31] considered the so-called false vacuum model with quartic potential. This model is characterised by two periods, where first the potential energy is dominated by a quartic term in the inflation, while at a certain moment a cosmological constant term takes over the leading role. In the transition period, there can be a short suspension of inflation, with related change in the EOS.

The index of EoS is defined as

$$\frac{P}{\rho} = \frac{-\dot{\rho} = 2 \dot{V}}{-\dot{\rho} = 2 + \dot{V}} \quad (48)$$

where we for simplicity have assumed a single field model. The evolution equation for the field is a second order equation, and it is clear that a change in the EoS only can be sourced by a change in the potential energy. In all cases  $V$  diminishes. Because of the equation of motion

$$+ 3H \dot{\phi} + V' = 0 \quad (49)$$

this leads to a large second order derivative and the inflaton enters a stage of fast-roll, where approximately

$$+ 3H \dot{\phi} = 0 \quad (50)$$

After some time the balance between the friction term and the source term  $V'$  is reestablished. Looking at (5) and (44) we can estimate that a significant change in power spectrum will only happen when

$$\frac{4V}{9H^2} \approx 1 \quad (51)$$

for at least one e-fold. Supposing that  $V'$  during one e-fold is diminished by a factor  $\epsilon$ , the average change during this period is

$$\frac{dV}{dN} = (1 - \epsilon)V = 3(1 - \epsilon)H^2 \quad (52)$$

Using the last two equations we find a bound on

$$\frac{1}{4} \quad (53)$$

It is clear that these are very rough estimates, but it does show that to get a significant change in the power spectrum of the fluctuations a rather large change in  $V'$  is required. This could either be due to interactions with other fields, as in our case, or due to the internal dynamics of the model, as in the two mentioned cases.

## 4. Observational data

### 4.1. Cosmic microwave background

The CMB temperature fluctuations are conveniently described in terms of the spherical harmonics power spectrum

$$C_l = \langle |h_{lm}|^2 \rangle \quad (54)$$

where

$$\frac{T}{T}(\theta, \phi) = \sum_{lm} a_{lm} Y_{lm}(\theta, \phi) \quad (55)$$

Since Thomson scattering polarizes light, there are additional power spectra coming from the polarization anisotropies. The polarization can be divided into a curl-free (E)

and a curl ( $B$ ) component, yielding four independent power spectra:  $C_{T;l}$ ;  $C_{E;l}$ ;  $C_{B;l}$  and the temperature  $E$ -polarization cross-correlation  $C_{TE;l}$ .

The WMAP experiment have reported data only on  $C_{T;l}$  and  $C_{TE;l}$ , as described in Ref. [1, 2, 3, 4, 5]

We have performed the likelihood analysis using the prescription given by the WMAP collaboration which includes the correlation between different  $C_l$ 's [1, 2, 3, 4, 5]. Foreground contamination has already been subtracted from their published data.

In parts of the data analysis we also add other CMB data from the compilation by Wang et al. [82] which includes data at high  $l$ . Altogether this data set has 28 data points.

## 4.2. Large scale structure

The 2dF Galaxy Redshift Survey (2dFGRS) [48] has measured the redshifts of more than 230 000 galaxies with a median redshift of  $z_m = 0.11$ . One of the main goals of the survey was to measure the galaxy power spectrum on scales up to a few hundred Mpc, thus filling in the gap between the small scales covered by earlier galaxy surveys and the largest scales where the power spectrum is constrained by observations of the CMB. A sample of the size of the 2dFGRS survey allows large-scale structure statistics to be measured with very small random errors. An initial estimate of the convolved, redshift-space power spectrum of the 2dFGRS has been determined [11] for a sample of 160 000 redshifts. On scales  $0.02 < k < 0.15 h \text{ Mpc}^{-1}$  the data are robust and the shape of the power spectrum is not affected by redshift-space or nonlinear effects, though the amplitude is increased by redshift-space distortions. A potential complication is the fact that the galaxy power spectrum may be biased with respect to the matter power spectrum, i.e. light does not trace mass exactly at all scales. This is often parametrised by introducing a bias factor

$$b^2(k) = \frac{P_g(k)}{P_m(k)}; \quad (56)$$

where  $P_g(k)$  is the power spectrum of the galaxies, and  $P_m(k)$  is the matter power spectrum. Indeed it is well established that on scales less than  $\sim 10 \text{ Mpc}$  different galaxy populations exhibit different clustering amplitudes, the so-called morphology-density relation (see e.g. [49, 50, 51, 52]). Hierarchical merging scenarios also suggest a more complicated picture of biasing as it could be non-linear, scale-dependent and stochastic [53, 54, 55, 56, 57, 58]. However, analysis of the semi-analytic galaxy formation models in [59], as well as the simulations in [57] suggest that the biasing is simple and scale-independent on large scales  $k > 0.15 h \text{ Mpc}^{-1}$  where the power spectrum is well described by linear theory, and we restrict our analysis of the 2dFGRS power spectrum to these scales. Two different analyses have demonstrated that the 2dFGRS power spectrum is consistent with linear, scale-independent bias [61, 62]. Thus, the shape of the galaxy power spectrum can be used straightforwardly to constrain the shape of the matter power spectrum on large scales.

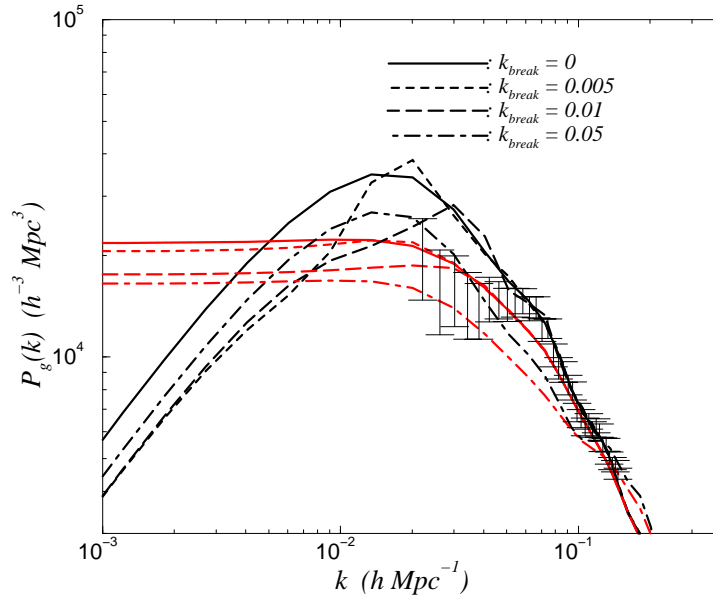


Figure 3. The effect of convolving matter power spectra with the 2dFGRS window function. The black lines are the matter power spectra computed with CMBFAST for four different values of  $k_{\text{break}}$ , the red lines are the corresponding spectra after convolution with the window function. The vertical bars are the 2dFGRS power spectrum data points.

When looking for steps or other features in the primordial power spectrum using the 2dFGRS, one should bear in mind that what is measured is the convolution of the true galaxy power spectrum with the 2dFGRS window function [11],

$$P_{\text{conv}}(k) = \int_0^z P_g(k - q) W_k(q) d^3q; \quad (57)$$

where  $W$  is the window function. In an earlier, simplified attempt to look for steps in the primordial power spectrum [63] it was found that the window function of the 2dFGRS more or less washed out any features in the primordial power spectrum for comoving momenta  $k < 0.1 h \text{ Mpc}^{-1}$ . The effect on the class of models considered in the present paper is illustrated in figure 3 for four different values of  $k_{\text{break}}$ . However, combining the 2dFGRS power spectrum with CMB data breaks parameter degeneracies that are present if each dataset is analysed separately, and therefore a combination of large-scale structure and CMB data gives tighter constraints on the primordial power spectrum than the CMB alone.

## 5. Likelihood analysis

For calculating the theoretical CMB and matter power spectra we use the publicly available CMBFAST package [44]. As the set of cosmological parameters we choose

parameter	prior	
$\Omega_m$	0:28	0:14 (Gaussian)
$h$	0:72	0:08 (Gaussian)
$\Omega_b h^2$	0:014	0:040 (Top Hat)
$n_s$	0:6	1:4 (Top hat)
$\tau$	0	1 (Top hat)
$Q$		free
$b$		free

Table 1. The different priors on parameters other than  $N_e$  and  $k_{b\text{reak}}$  used in the likelihood analysis.

$\Omega_m$ , the matter density,  $\Omega_b$ , the baryon density,  $H_0$ , the Hubble parameter,  $n_s$ , the scalar spectral index of the primordial fluctuation spectrum,  $\tau$ , the optical depth to reionization,  $Q$ , the normalization of the CMB power spectrum,  $b$ , the bias parameter, and finally the two parameters related to the step height,  $N_e$ , and location ( $k_{b\text{reak}}$ ). We restrict the analysis to geometrically flat models  $\Omega_m + \Omega_b = 1$ .

In principle one might include even more parameters in the analysis, such as  $r$ , the tensor to scalar ratio of primordial fluctuations. However,  $r$  is most likely so close to zero that only future high precision experiments may be able to measure it. The same is true for other additional parameters. Small deviations from slow-roll during inflation can show up as a logarithmic correction to the simple power-law spectrum predicted by slow-roll. [45, 46, 47] or additional relativistic energy density [64, 65, 66, 67, 68, 69, 70, 71, 72] could be present. However, there is no evidence of any such effect in the present data and therefore we restrict the analysis to the "minimal" standard cosmological model.

In this full numerical likelihood analysis we use the free parameters discussed above with certain priors determined from cosmological observations other than CMB and LSS. In flat models the matter density is restricted by observations of Type Ia supernovae to be  $\Omega_m = 0.28 \pm 0.14$  [74]. The current estimated range for  $\Omega_b h^2$  from BBN is  $\Omega_b h^2 = 0.020 \pm 0.002$  [76], and finally the HST Hubble key project has obtained a constraint on  $H_0$  of  $72 \pm 8 \text{ km s}^{-1} \text{ Mpc}^{-1}$  [75]. The actual marginalization over parameters other than  $N_e$  and  $k_{b\text{reak}}$  was performed using a simulated annealing procedure [77].

In Fig. 4 we show results of the likelihood calculation for various different data sets. In panel (a) results are shown for an analysis with all available data, WMAP, the Wang et al. compilation (Wang), and the 2dFGRS power spectrum. In panel (b) we show results for WMAP + Wang, in panel (c) for WMAP + 2dFGRS, and finally in panel (d) for WMAP data only. The figure shows the 68% and 95% exclusion limits for the parameters  $N_e$  and  $k_{b\text{reak}}$ . These two contours correspond to  $\chi^2 = 2.31$  and  $\chi^2 = 6.17$  respectively. Best fit values and number of degrees of freedom for each of the four cases are tabulated in Table 2.

Several things can be noted from this figure. First, the 2dFGRS power spectrum

case	$\chi^2$	d.o.f.	$\chi^2/\text{d.o.f.}$
(a)	1466.9	1388	1.057
(b)	1459.2	1371	1.064
(c)	1440.9	1360	1.059
(d)	1432.2	1343	1.065

Table 2. Best  $\chi^2$  and number of degrees of freedom for each of the cases shown in Fig. 4.

only constrains a step-like feature on scales smaller than  $k \approx 0.05 - 0.1 \text{ h Mpc}^{-1}$  because the window function of the survey washes out any features on scales larger than this.

Second, the CMB data are mainly sensitive to scales corresponding to  $l \approx 50 - 100$ , and only to a lesser extent to features at high  $l$ . The main reason for this is that CMB data does not directly probe the primordial power spectrum, but rather the primordial spectrum convolved with an effective window function. This will be discussed in detail in the next subsection. The result of the convolution is that a sharp step in  $P(k)$  appears as a gradual increase in power over a range in  $l$  in the CMB spectrum. It is relatively easy to mask this effect by changing other cosmological parameters. However, scales at  $l < 100$  were outside the particle horizon at recombination and therefore much less sensitive to changes in most of the cosmological parameters. This is the reason why the likelihood analysis shows a very stringent bound in this range, and not in the region around the first acoustic peak, as could perhaps have been expected.

Finally, adding the Wang et al. compilation to the WMAP data significantly tightens the bound on  $N_e$  over most of the range in  $k$ -space, particularly of course at the smaller scales where the WMAP data suffer from finite angular resolution. However, in some parts of parameter space the constraint actually becomes slightly worse by adding other CMB data. This is not inconsistent, it just means that the Wang et al. data actually favours a small step and therefore pushes the total likelihood towards higher values of  $N_e$ .

In the last panel the effect of the finite resolution of the WMAP data becomes apparent beyond  $k \approx 0.05 \text{ h Mpc}^{-1}$ , corresponding to  $l \approx 450$ , exactly around the scale where the error bars are no longer cosmic variance limited.

Finally, we note that our analysis is restricted to geometrically flat models. However, since spatial geometry affects the CMB spectrum at scales  $l < 100$  it is possible that the accuracy with which we have constrained  $N_e$  on this scale has been slightly overestimated.

### 5.1. The CMB window function

CMB data do not directly measure the underlying primordial power spectrum of fluctuations. Rather, they measure the spectrum folded with a transfer function in

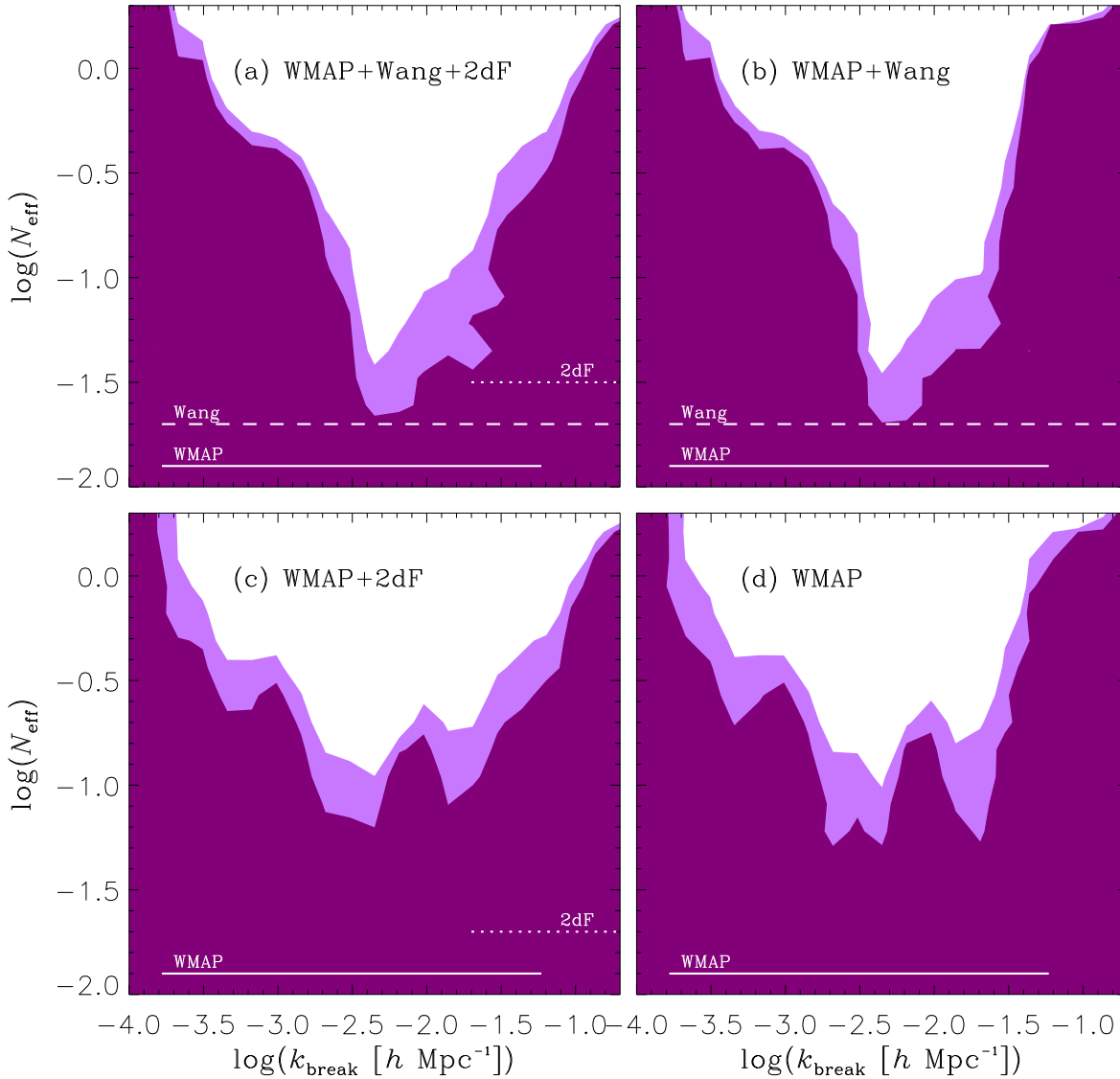


Figure 4. 68% and 95% confidence exclusion plot of the parameters  $N_{\text{eff}}$  and  $k_{\text{break}}$  for the four different cases described in the text. The horizontal lines show the range in  $k$ -space covered by various data sets. CMB data have been converted from  $k$  to  $l$  using the approximate prescription  $l \approx 2k = H_0$ .

the following sense

$$C_1 = \int_0^z \frac{dk}{k} P(k) \frac{1}{z_1} \frac{1}{z_1}(k); \quad (58)$$

where  $\frac{1}{z_1}(k)$  is the transfer function taken at the present,  $z = 0$ , where  $z$  is conformal time. Following the line-of-sight approach pioneered by Seljak and Zaldarriaga [44] this transfer function can be written as

$$\frac{1}{z_1}(k) = \int_0^0 dS(k; z) j_1(k(z - z_0)); \quad (59)$$

where  $S$  is a source function, calculated from the Boltzmann equation, and  $j_1(x)$  is a spherical Bessel function. However, in order to get a very rough idea about the effective

window function  $w_1(k) = \int_{l_0}^2(k) dk$  of CMB we approximate  $S$  with a constant to obtain

$$w_1(k) / \int_{l_0}^2(k) dk = \begin{cases} \frac{k_0}{l_0} & \text{for } k_0 < l_0 \\ \frac{1}{k^3} & \text{for } k_0 > l_0 \end{cases} \quad (60)$$

This simple equation shows several things: (a) A feature at some specific wavenumber  $k = k_0$  has the greatest impact on the CMB spectrum at  $l \sim k_0$ . For a matter dominated universe,  $l_0 = H_0 = 2$ , yielding  $l \sim 2k_0 = H_0$ . (b) The CMB window function is quite broad, and narrow features in  $P(k)$  are accordingly difficult to detect.

In the present model the main detectable feature is a step in the power spectrum, characterized by the amplitude,  $N_e$ , and the location,  $k_{\text{break}}$ . Adding such a step to an otherwise scale-invariant spectrum yields a primordial power spectrum

$$P(k) = A + N_e \theta(k - k_{\text{break}}) \quad (61)$$

Calculating  $C_l$  from Eq. 58, using the window function Eq. 60 then gives us

$$C_l / \int_{l_0}^2(k) dk = \begin{cases} \frac{A + N_e}{(l_0)^2} & \text{for } k_{\text{break}} < l_0 \\ \frac{A}{(l_0)^2} + \frac{N_e}{k_{\text{break}}^2} & \text{for } k_{\text{break}} > l_0 \end{cases} \quad (62)$$

Finally, we can define the ratio,  $R$ , between the CMB spectrum with the step, and one with exactly the same cosmological parameters, but without the step

$$R = \begin{cases} 1 + \frac{N_e}{A} & \text{for } k_{\text{break}} < l_0 \\ 1 + \frac{N_e}{A} \frac{l_0^2}{k_{\text{break}}^2} & \text{for } k_{\text{break}} > l_0 \end{cases} \quad (63)$$

In Fig. 5 we show the ratio of two spectra calculated with CMBFAST. The first model is a standard  $\Omega_m = 1$  CDM model with  $h = 0.7$  and scale-invariant initial spectrum,  $P(k) = A$ . The second model is with the same parameters, but with a step added with parameters  $N_e = A$  and  $k_{\text{break}} = 0.05 \text{ Mpc}^{-1}$ . The full line shows the numerical result, and the dashed line shows the approximation from Eq. 63. Clearly our very simple approximation still captures the essential impact of a step-like feature on the CMB spectrum.

The conclusion is that the effective window function  $w_1(k)$  for CMB smoothes out the step feature in the underlying primordial power spectrum  $P(k)$ . This in turn means that the ability of CMB data to detect step-like features is significantly degraded.

A feature which is at first surprising is that the constraint on the step amplitude  $N_e$  is strongest at  $k_{\text{break}} = 0.01$ , corresponding to  $l \sim 90$  which is significantly above the scale of the first acoustic peak. The reason is that scales above  $l \sim 100$  were outside the particle horizon at recombination and therefore the CMB spectrum at these scales is not susceptible to acoustic oscillation effects which can otherwise mask a step in the

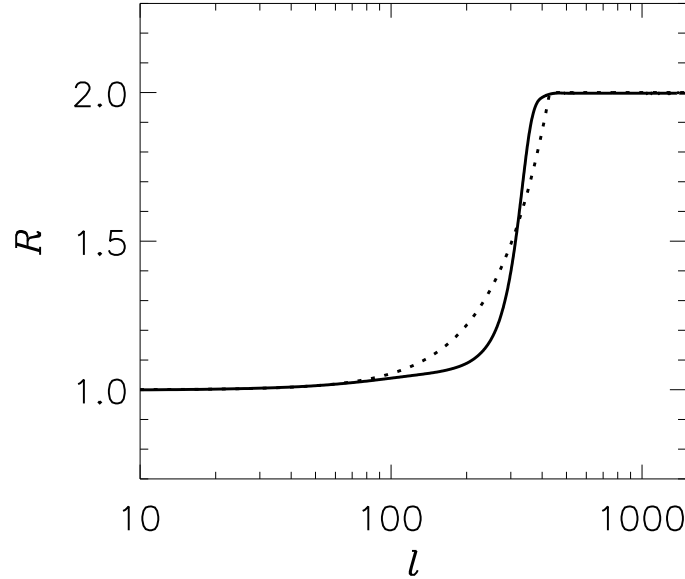


Figure 5. Ratio of  $C_1$  for model with step to model without step. The full line is the precise numerical calculation and the dashed is the approximation in Eq. 63.

primordial spectrum. At  $l < 30$  the constraint on  $N_e$  becomes gradually weaker simply because cosmic variance increases the error bars on  $C_1$ . Clearly, even though the present CMB data is most sensitive to step features at scales corresponding to  $l \approx 50 - 100$  a future experiment like Planck which is cosmic variance limited out to  $l > 2000$  would be able to put strong constraints on  $N_e$  at much higher  $l$ , simply because the greater measurement accuracy would break the degeneracy between a step and changes in other cosmological parameters.

## 6. Discussion

We have presented a calculation of the perturbation to the power spectra that is generated under inflation due to a resonant coupling of the inflaton to a boson. The calculation has been made only under the assumption of slow-roll evolution of the inflaton before and after the interaction, but no constraints have been put on the specific form of the potential. In [10] the same setup was studied, but with a trilinear coupling to a fermion field. Our results for the perturbation to the primordial power spectrum are dramatically different to their findings. A step-like feature is formed, and on top of this, to the ultraviolet side of the step, there is a highly oscillating transient. For weak couplings the size of the step scales like  $g^{5=2}N$  and a suppression of power on large scales is observed, while at larger values of the coupling this simple relation breaks down and we can have both suppression and enhancement of the large scale power relative to the ultraviolet part.

The differences we observe with respect to the results of Chung et al [10] are easily explained from the more limited analysis they performed. Indeed similar numerical studies support our conclusion. Easther et al [12] have investigated the impact from a step in the potential of the inflation and found a very similar feature. They reproduce the oscillations seen in our model, but no significant amplification is observed. Leach et al undertook a detailed investigation of the false vacuum model [34] where they found a suppression of the infrared part of the spectrum caused by changes in the entropy perturbation very much like the one we observe. Starobinsky [35] explored the very simplest model, where the inflationary potential has a step, and reached the same conclusion. Common for all studies is that the effects seen are due to the self contained dynamics of the field, while in our model it is caused by the mutual interaction between the inflation and external fields. This is a major difference, and while the other models requires fine tuning of the potential, such that the "feature" occurs in the small range accessible to observational cosmology, our model can be naturally supported in the context of supersymmetric theories with extra dimensions or superstring theories. These theories can have a whole hierarchy of particles with masses comparable to the Planck mass [32, 10, 33]. It would then be much more natural to expect at least one particle with parameters, such that the produced feature falls into the range open to observations [8]. Nonetheless, the presented model should be understood as a realistic toy model, while a real model should have some basis in particle physics.

It would have been desirable to do a full numerical study including higher order metric terms coming from the gravitational interaction of the fields. We think, though, that the overall features of the phenomena are correctly described in this analysis. It can be argued, that because the particles are produced relativistically and the peak wave number is very large in comparison with the Hubble horizon at that epoch, the process should be causal in nature, and therefore not much dependent on the expansion of the universe.

One feature we did miss in our study, which could be important, is the quantum treatment of the inflation fluctuations and the possibility of cross correlations between the fields. The step feature is largely due to the backreaction of the coupled particle directly on the inflation fluctuations, and therefore the cross correlation could be almost maximal. This leads to the possibility, that some of the energy contained in the inflation fluctuations oscillate into fluctuations in the other species and is redshifted away [30]. This clearly has to be addressed in a future study.

Using the recently published WMAP data together with other CMB data compiled by Wang et. al and large scale data from the 2dF Galaxy Redshift Survey we have found new upper limits on a break in the primordial power spectrum. We made a full likelihood analysis, and our conclusions are robust: The derived limits changed only slightly while varying the amount of data put into the analysis. We find that on scales  $k \approx 0.001 - 0.03 \text{ hMpc}^{-1}$  the 2 $\sigma$  upper limit on  $N_{\text{eff}}$  (the relative step height) is  $< 0.3$ . This conclusion is not sensitive to the chosen compilation of data and can essentially be derived from the WMAP data only. We also note that the CMB

spectrum is mainly sensitive to features at scales corresponding to  $l \sim 50 - 100$  and only to a lesser extent features at high  $l$ . This is because scales at  $l < 100$  were outside the particle horizon at recombination and much less affected by changes in most of the cosmological parameters. The constraint is significantly strengthened around  $l \sim 100$  by adding other data than WMAP. This is indirectly through their tightening of the limits on the cosmological parameters translating into less freedom to cancel the effect of a break around  $l \sim 50 - 100$ . While observations of the CMB gives us a wonderful tool to constrain the cosmology of our universe there is no a priori reason to expect a smooth, almost scale invariant power spectrum. The possibility of inherent noise and deviations in the primordial power spectrum gives us a promising possibility to probe the earliest history of our universe, but also have the potential of fooling cosmological parameter estimation at the percent level. One should remember this extra uncertainty of "unknown physics", when reading about limits set by new experiments. While so far there have been no trace of it, the deviation from full scale invariance and a possible bend in the power spectrum, as has been inferred by the WMAP team using their data, the 2dFGRS and Lyman $\alpha$  forest data, tells us that we are reaching levels of precision, where features could begin to crystallise out from the experimental errors.

It should be noted that our likelihood analysis for  $k_{\text{break}}$  and  $N_e$  is in fact quite general and can be applied to other models which produce a break in the power spectrum. Of course the oscillating behaviour of the spectrum close to the break is very specific to the present model, but the width of the window functions for both CMB and LSS tend to smear the oscillations so that the observational constraints are essentially on the step height and position.

Our result for  $(k_{\text{break}}; N_e)$  can therefore be compared for instance to the study of Ref. [83]. In that study it was found that the WMAP data shows a slight preference for a step in the power spectrum at  $k' \sim 2 - 3 \cdot 10^4 \text{ Mpc}^{-1}$ . In their analysis it was assumed that there was no power above the step scale, which in our language corresponds to  $N_{\text{eff}} \ll 1$ . In fact our WMAP-only analysis shows that the region where  $N_{\text{eff}} \ll 1$  and  $k_{\text{break}}' \sim 1.5 - 2.5 \cdot 10^4 \text{ Mpc}^{-1}$  provides a slightly better fit than no break. However, we find that this effect is not statistically significant.

Finally we note that our study only probes the scales measurable by CMB and LSS experiments. On much smaller scales limits on primordial black holes provide tight constraints on the primordial power spectrum (see for instance [84]) and can therefore be expected to provide interesting constraints on step-like features, constraining theories predicting the occurrence of particle production and phase transitions on a much wider range of scales.

## Acknowledgments

We acknowledge use of the publicly available CMBFAST package written by Uros Seljak and Matthias Zaldarriaga [44] and the use of computing resources at DCSC (Danish Center for Scientific Computing).

- [1] C. L. Bennett et al, *astro-ph/0302207*
- [2] D. N. Spergel et al, *astro-ph/0302209*
- [3] A. Kogut et al, *astro-ph/0302213*
- [4] G. Hinshaw et al, *astro-ph/0302217*
- [5] L. Verde et al, *astro-ph/0302218*
- [6] H. Peiris et al, *astro-ph/0302225*
- [7] D. La and P. J. Steinhardt, *Phys. Rev. Lett.* 62, 376 (1989)
- [8] J. A. Adams, G. G. Ross, and S. Sarkar, *Nucl. Phys. B* 503, 405 (1997)
- [9] A. A. Starobinsky, *Grav. Cosmol.* 4, 88 (1998)
- [10] D. J. H. Chung, E. W. Kolb, A. Riotto and I. I. Tkachev, *Phys. Rev. D* 62 043508 2000, [[arXiv:hep-ph/9910437](#)]
- [11] W. J. Percival et al. (the 2dFGRS team), *Mon. Not. R. Astron. Soc.* 327, 1297 (2001).
- [12] J. Adams, B. Cresswell and R. Easther", [[astro-ph/0102236](#)].
- [13] D. Wands, [[astro-ph/0201541](#)]. K. Malik, D. Wands and C. Ungarelli [[astro-ph/0211602](#)]. F. Di Marco, F. Finelli and R. Brandenberger [[astro-ph/0211276](#)].
- [14] L. F. Abbott and M. B. Wise", *Nucl. Phys. B* 244, 541-548 (1984).
- [15] E. D. Stewart and D. H. Lyth, *Phys. Lett. B* 302, 171-175 (1993), [[gr-qc/9302019](#)].
- [16] S. M. Leach, M. Sasaki, D. Wands and A. R. Liddle, [[astro-ph/0101406](#)].
- [17] L. R. W. Abramo, [[arXiv:gr-qc/9709049](#)].
- [18] J. Baacke, K. Heitmann and C. Patzold, *Phys. Rev. D* 581250131998, [[arXiv:hep-ph/9806205](#)].
- [19] J. Baacke and C. Patzold", *Phys. Rev. D* 62 084008 2000, [[arXiv:hep-ph/9912505](#)].
- [20] N. D. Birrell and P. C. W. Davies, *Quantum Fields in curved space time*, Cambridge University Press (1982).
- [21] M. B. P. Buni, S. M.atarrese, S. Mollerach and S. Sonego, *Class. Quant. Grav.* 14, 2585-2606 (1997), [[arXiv:gr-qc/9609040](#)]
- [22] D. Cormier, K. Heitmann and A. Mazumdar, [[arXiv:hep-ph/0105236](#)].
- [23] C. Gordon, D. Wands, B. A. Bassett and R. Maartens, *Phys. Rev. D* 63 023506 2001, [[arXiv:astro-ph/0009131](#)].
- [24] L. Kofman, A. Linde and A. A. Starobinsky, *Phys. Rev. D* 56 3258-3295 1997, [[arXiv:hep-ph/9704452](#)].
- [25] V. F. Mukhanov, H. A. Feldman and R. H. Brandenberger, *Phys. Rept.* 215, 203-333 (1992)
- [26] D. Wands, K. A. Malik, D. H. Lyth and A. R. Liddle, *Phys. Rev. D* 62 043527 2000, [[arXiv:astro-ph/0003278](#)].
- [27] G. Rigopoulos, [[arXiv:astro-ph/0212141](#)].
- [28] J. M. Aldecena, [[arXiv:astro-ph/0210603](#)].
- [29] V. Acquaviva, N. Bartolo, S. Matarrese, A. Riotto, [[arXiv:astro-ph/0209156](#)].
- [30] N. Bartolo, S. Matarrese and A. Riotto, *Phys. Rev. D* 64 083514, [[arXiv:astro-ph/0106022](#)].
- [31] D. Roberts, A. R. Liddle and D. H. Lyth, *Phys. Rev. D* 51, 4122-4128, 1995, [[arXiv:astro-ph/9411104](#)].
- [32] D. H. Lyth and A. Riotto, *Phys. Rept.* 314 1-146 1999, [[arXiv:hep-ph/9807278](#)]
- [33] K. A. Malik, [[arXiv:astro-ph/0101563](#)]
- [34] S. M. Leach and A. R. Liddle, *Phys. Rev. D* 63 043580 2001, [[arXiv:astro-ph/0010082](#)]
- [35] A. A. Starobinsky, *JETP Lett.* 42, 51 (1985)
- [36] C. L. Bennett et al, *Astrophys. J.* 464 1 1996 [[astro-ph/9601067](#)].
- [37] C. B. Netterfeld et al. [Boomerang Collaboration], [[arXiv:astro-ph/0104460](#)].
- [38] A. T. Lee et al, [[arXiv:astro-ph/0104459](#)].
- [39] N. W. Halverson et al, [[arXiv:astro-ph/0104489](#)].
- [40] X. Wang, M. Tegmark and M. Zaldarriaga, [[arXiv:astro-ph/0105091](#)] (W T Z).
- [41] X. Yu et al, [[arXiv:astro-ph/0010552](#)].
- [42] J. Peacock et al, *Nature* 410, 169 (2001).
- [43] M. Tegmark, A. J. S. Hamilton and Y. Xu, [[arXiv:astro-ph/0111575](#)]

- [44] U. Seljak and M. Zaldarriaga, *Astrophys. J.* 469, 437 (1996).
- [45] S. Hannestad, S. H. Hansen and F. L. Villante, *Astropart. Phys.* 16, 137 (2001) [[arXiv:astro-ph/0012009](#)].
- [46] S. Hannestad, S. H. Hansen, F. L. Villante and A. J. Hamilton, *Astropart. Phys.* 17, 375 (2002) [[arXiv:astro-ph/0103047](#)].
- [47] L. M. Gri ths, J. Silk and S. Zaroubi, [astro-ph/0010571](#).
- [48] M. Colless et al. (the 2dFGRS team ), *Mon. Not. R. Astron. Soc.* 328, 1039 (2001).
- [49] Dressler A, *Galaxy morphology in rich clusters*{Implications for the formation and evolution of galaxies, 1980, *Astrophys. J.* 236 351.
- [50] Hem it S, Santiago B X, Lahav O, Strauss M A, Davis M, Dressler A and Huchra J P, 1996, *Mon. Not. R. Astron. Soc.* 283 709 [[astro-ph/9608001](#)]
- [51] Norberg P et al. (the 2dFGRS team ), *The 2dF Galaxy Redshift Survey: the dependence of galaxy clustering on luminosity and spectral type*, 2002 *Mon. Not. R. Astron. Soc.* 332 827 [[astro-ph/0112043](#)]
- [52] Zehavi I et al. (SDSS Collaboration), 2002 *Astrophys. J.* 571 172 [[astro-ph/0106476](#)]
- [53] Mo H J and White S D M, 1996 *Mon. Not. R. Astron. Soc.* 282 347 [[astro-ph/9512127](#)]
- [54] Matarrese S, Coles P, Lucchin F and Moscardini L, 1997 *Mon. Not. R. Astron. Soc.* 286 115 [[astro-ph/9608004](#)]
- [55] M agliocchetti M, Bagla J, Maddox S J and Lahav O, 2000 *Mon. Not. R. Astron. Soc.* 314 546 [[astro-ph/9902260](#)]
- [56] Dekel A and Lahav O, 1999 *Astrophys. J.* 520 24 [[astro-ph/9806193](#)]
- [57] Blanton M, Cen R, Ostriker J P, Strauss M A and Tegmark M, 2000 *Astrophys. J.* 531 1 [[astro-ph/9903165](#)]
- [58] Somerville R, Lemson G, Sigad Y, Dekel A, Colberg J, Kau mann G and White S D M, 2001 *Mon. Not. R. Astron. Soc.* 320 289 [[astro-ph/9912073](#)]
- [59] Berlind A A, Weinberg D H, Benson A J, Baugh C M, Cole S, Dav e R, Frenk C S, Katz N and Lacey C G, 2002 *Preprint astro-ph/0212357*
- [60] G . P. Efstathiou et al. (the 2dFGRS team ), *Mon. Not. R. Soc.* 330, L29 (2002).
- [61] O . Lahav et al. (the 2dFGRS team ), *Mon. Not. R. Soc.* 333, 961 (2002).
- [62] L. Verde et al. (the 2dFGRS team ), *Mon. Not. R. Soc.* 335, 432 (2002)
- [63] Elgar y, Gramann M and Lahav O, 2002 *Mon. Not. R. Astron. Soc.* 333 93 [[astro-ph/0111208](#)]
- [64] G . Jungman, M . Kam ionkowski, A . Kosowsky and D . N . Spergel, *Phys. Rev. D* 54, 1332 (1996) [[arXiv:astro-ph/9512139](#)].
- [65] J. Lesgourgues and M . Peloso, *Phys. Rev. D* 62, 081301 (2000) [[arXiv:astro-ph/0004412](#)].
- [66] S. Hannestad, *Phys. Rev. Lett.* 85, 4203 (2000) [[arXiv:astro-ph/0005018](#)].
- [67] S. Esposito, G . Mangano, A . M elchiorri, G . M iele and O . Pisanti, *Phys. Rev. D* 63, 043004 (2001) [[arXiv:astro-ph/0007419](#)].
- [68] J. P. Kneller, R. J. Scherrer, G . Steigman and T . P . Walker, *Phys. Rev. D* 64, 123506 (2001) [[arXiv:astro-ph/0101386](#)].
- [69] S. Hannestad, *Phys. Rev. D* 64, 083002 (2001) [[arXiv:astro-ph/0105220](#)].
- [70] S. H . Hansen, G . Mangano, A . M elchiorri, G . M iele and O . Pisanti, *Phys. Rev. D* 65, 023511 (2002) [[arXiv:astro-ph/0105385](#)].
- [71] R. Bowen, S. H . Hansen, A . M elchiorri, J. Silk and R . Trotta, [arXiv:astro-ph/0110636](#).
- [72] A . D . Dolgov, S. H . Hansen, S. Pastor, S. T. Petcov, G . G . Ra elt and D . V . Sem ikoz, [arXiv:hep-ph/0201287](#).
- [73] V . R . Eke, S. Cole and C . S . Frenk, [arXiv:astro-ph/9601088](#).
- [74] S. Perlm utter et al. [Supernova Cosm ology Project Collaboration], *Astrophys. J.* 517, 565 (1999) [[arXiv:astro-ph/9812133](#)].
- [75] W . L . Freedman et al., *Astrophys. J. Lett.* 553, 47 (2001).
- [76] S. Burles, K . M . Nollett and M . S . Turner, *Astrophys. J.* 552, L1 (2001) [[arXiv:astro-ph/0010171](#)]; see also K . A . Olive, G . Steigman and T . P . Walker, *Phys. Rept.* 333, 389 (2000)

- [arXiv:astro-ph/9905320] for a recent review
- [77] S. Hannestad, *Phys. Rev. D* **61**, 023002 (2000).
- [78] A. J. S. Hamilton and M. Tegmark, *Mon. Not. R. Astron. Soc.* **330**, 506 (2002).
- [79] See the SDSS homepage <http://www.sdss.org/>
- [80] See the MAP homepage <http://map.gsfc.nasa.gov/>
- [81] .Elgaray et al, *Phys. Rev. Lett.* **89** 061303, arXiv:astro-ph/0204152.
- [82] X. Wang, M. Tegmark, B. Jain and M. Zaldarriaga, arXiv:astro-ph/0212417.
- [83] S. L. Bridle, A. M. Lewis, J. Weller and G. Efstathiou, arXiv:astro-ph/0302306.
- [84] T. Bringmann, C. Kiefer and D. Polarski, *Phys. Rev. D* **65**, 024008 (2002) [arXiv:astro-ph/0109404].